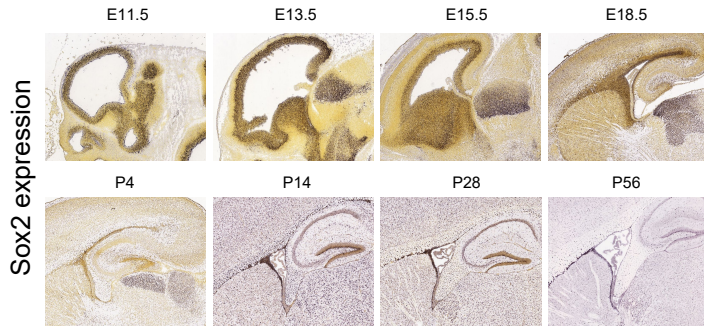
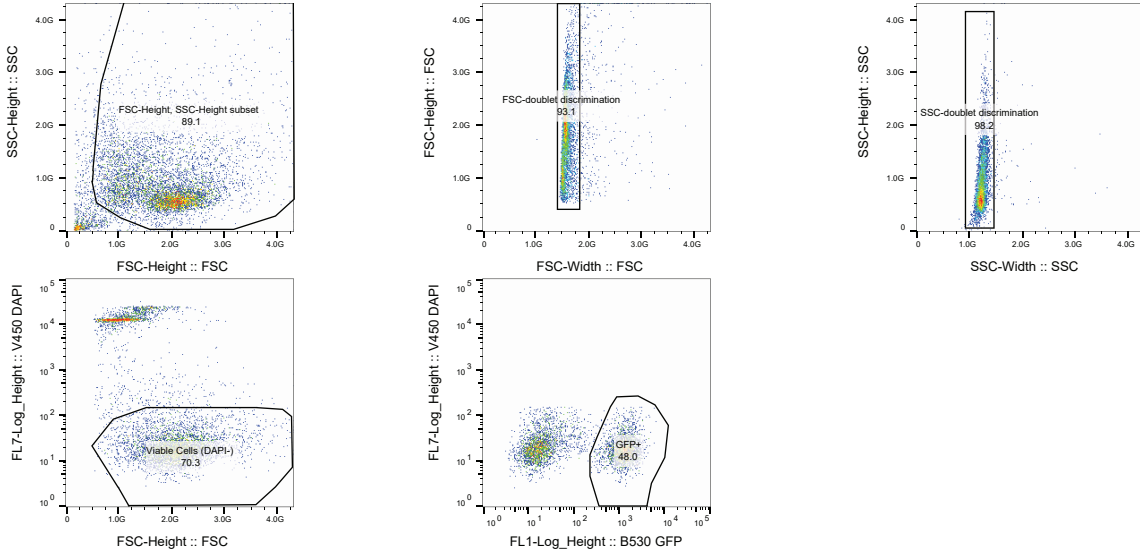
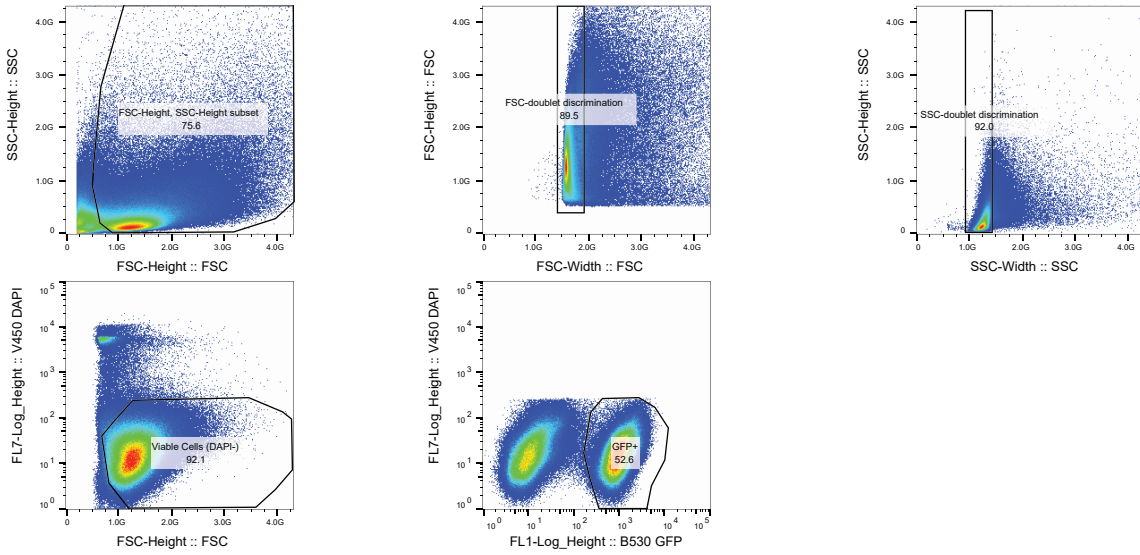
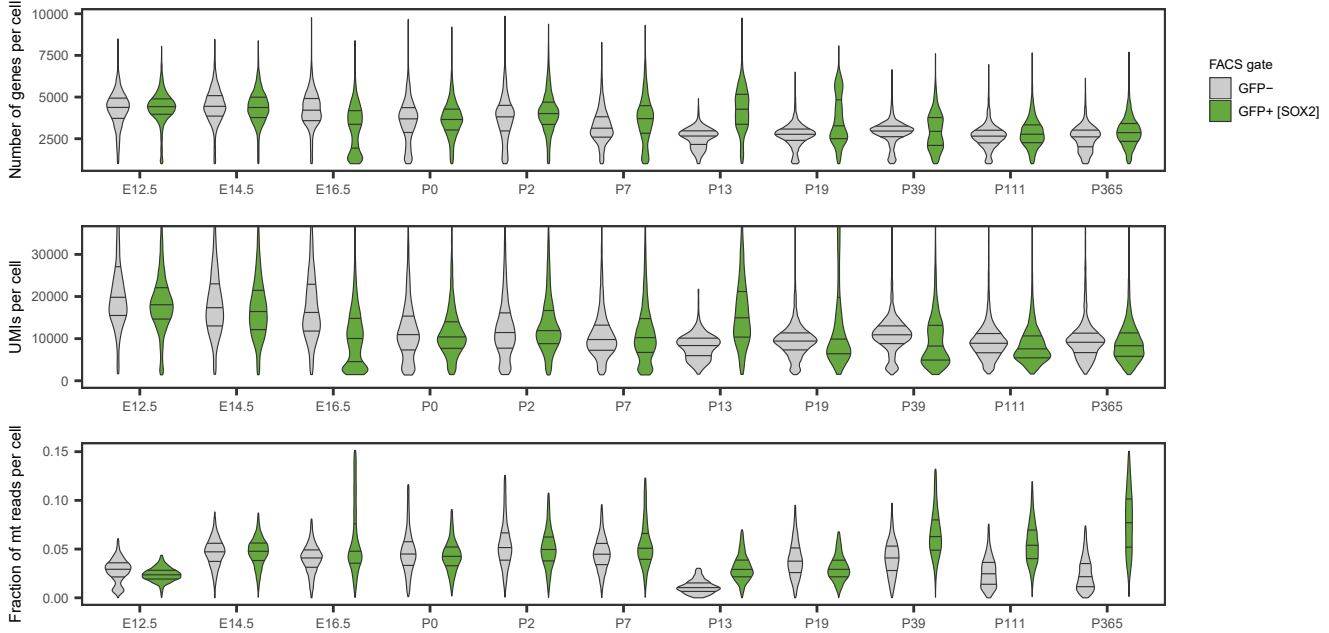
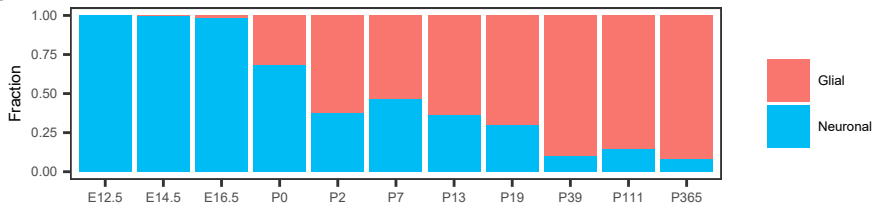
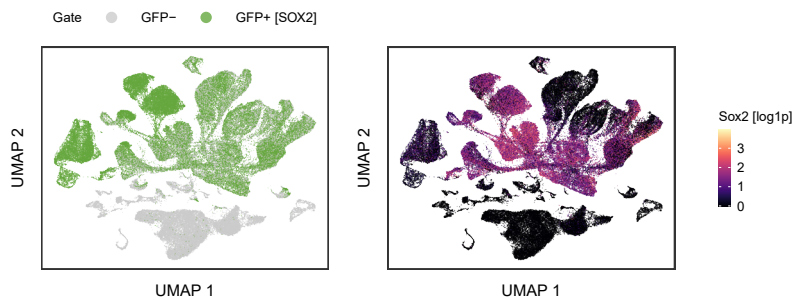
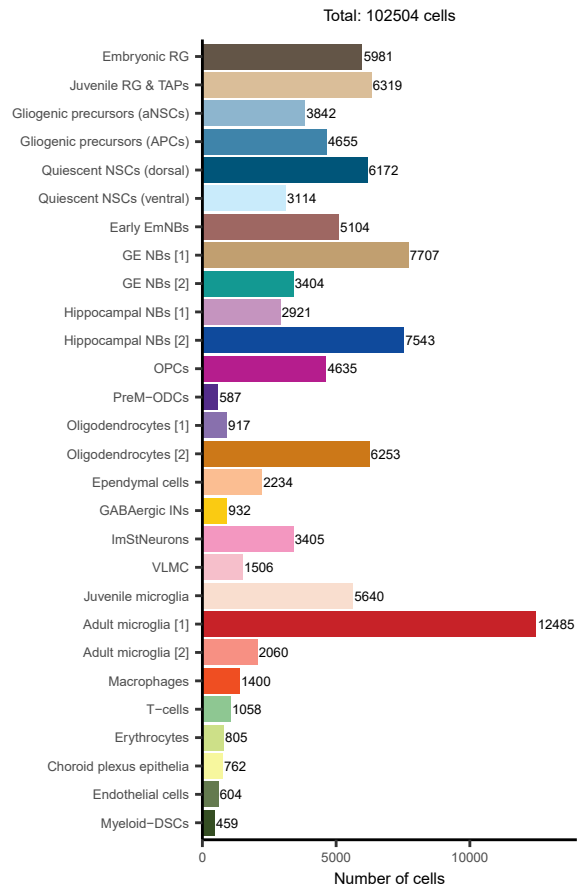


a**b****c**

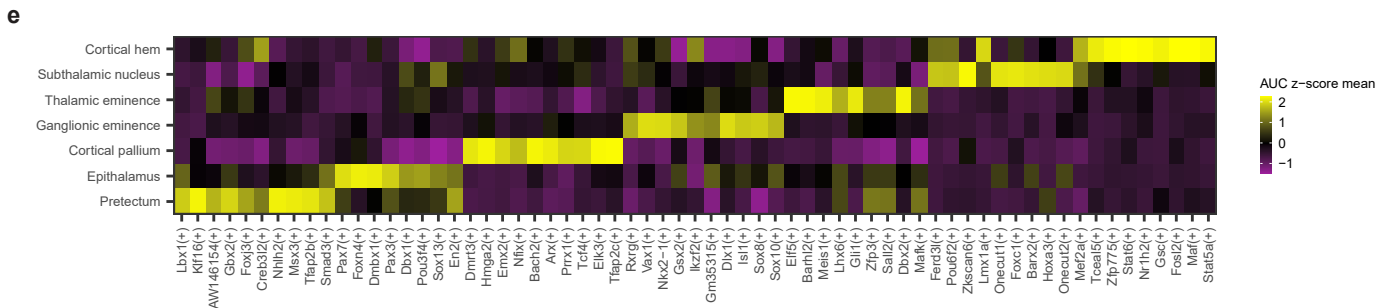
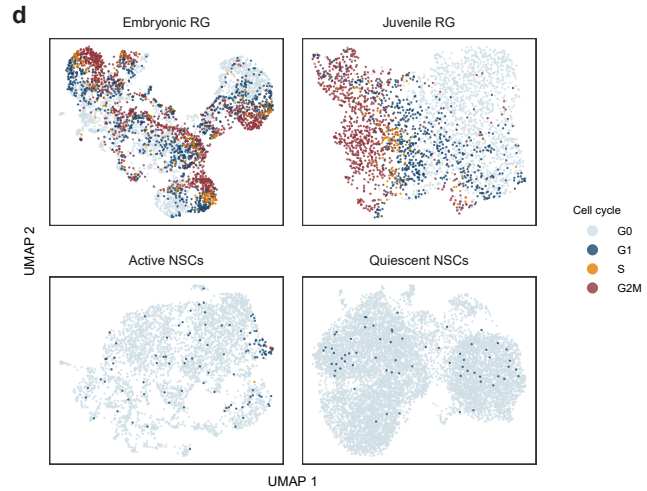
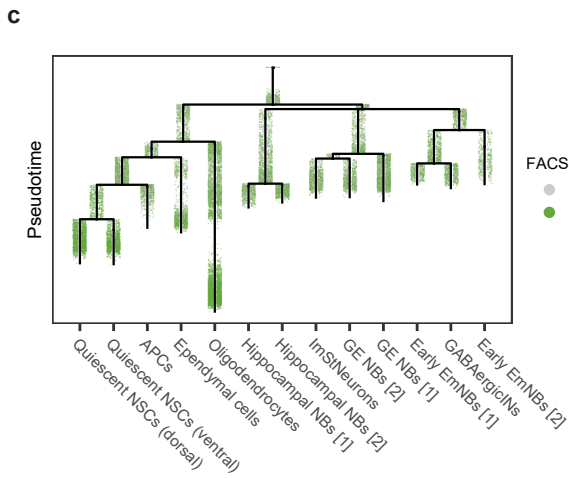
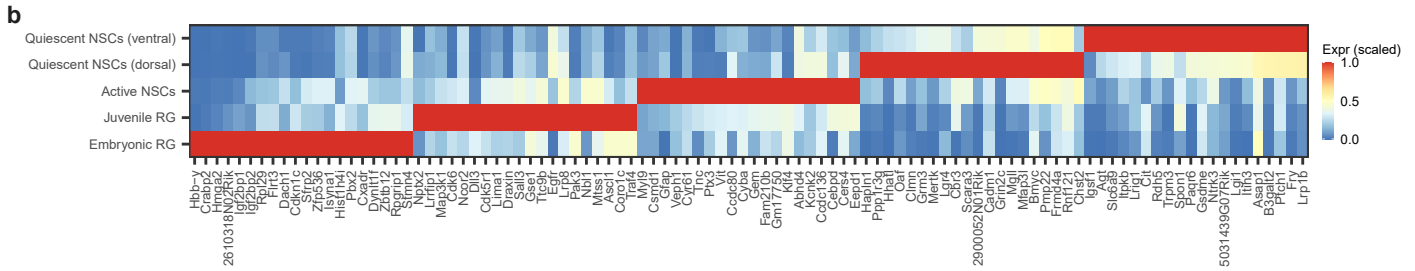
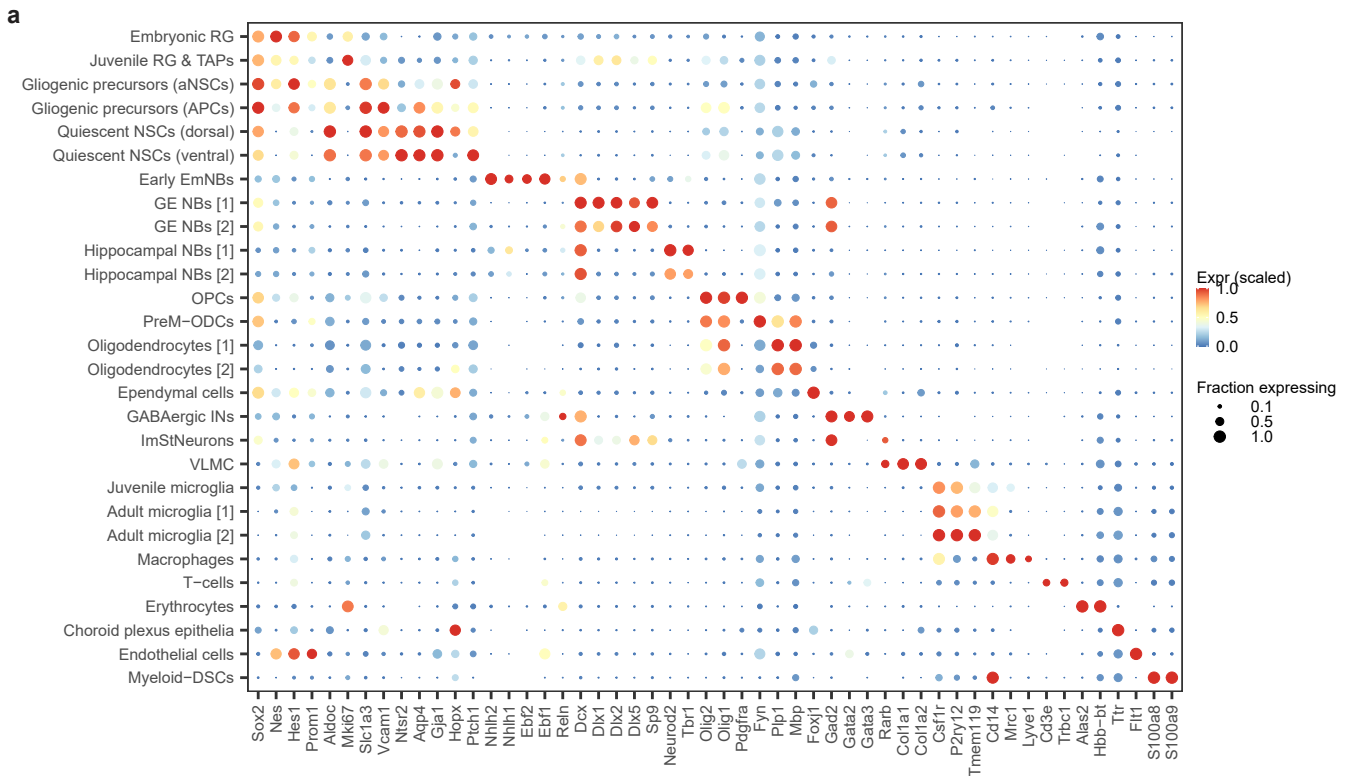
Supplementary Fig. 1 | The expression of Sox2 across cerebral development and the FACS gating strategy. a, In-situ hybridization staining of sagittal embryo/adult brain slices showing the expression of Sox2 across 8 developmental timepoints. In-situ hybridization images were obtained from the Allen Brain Map: Developing Mouse Brain Atlas. **b, c**, FACS plots of the collection strategy of the GFP^{+/-} cells from embryonic day E12.5 (b) and postnatal day 2 (c) *Sox2eGFP* mouse brain samples.

a

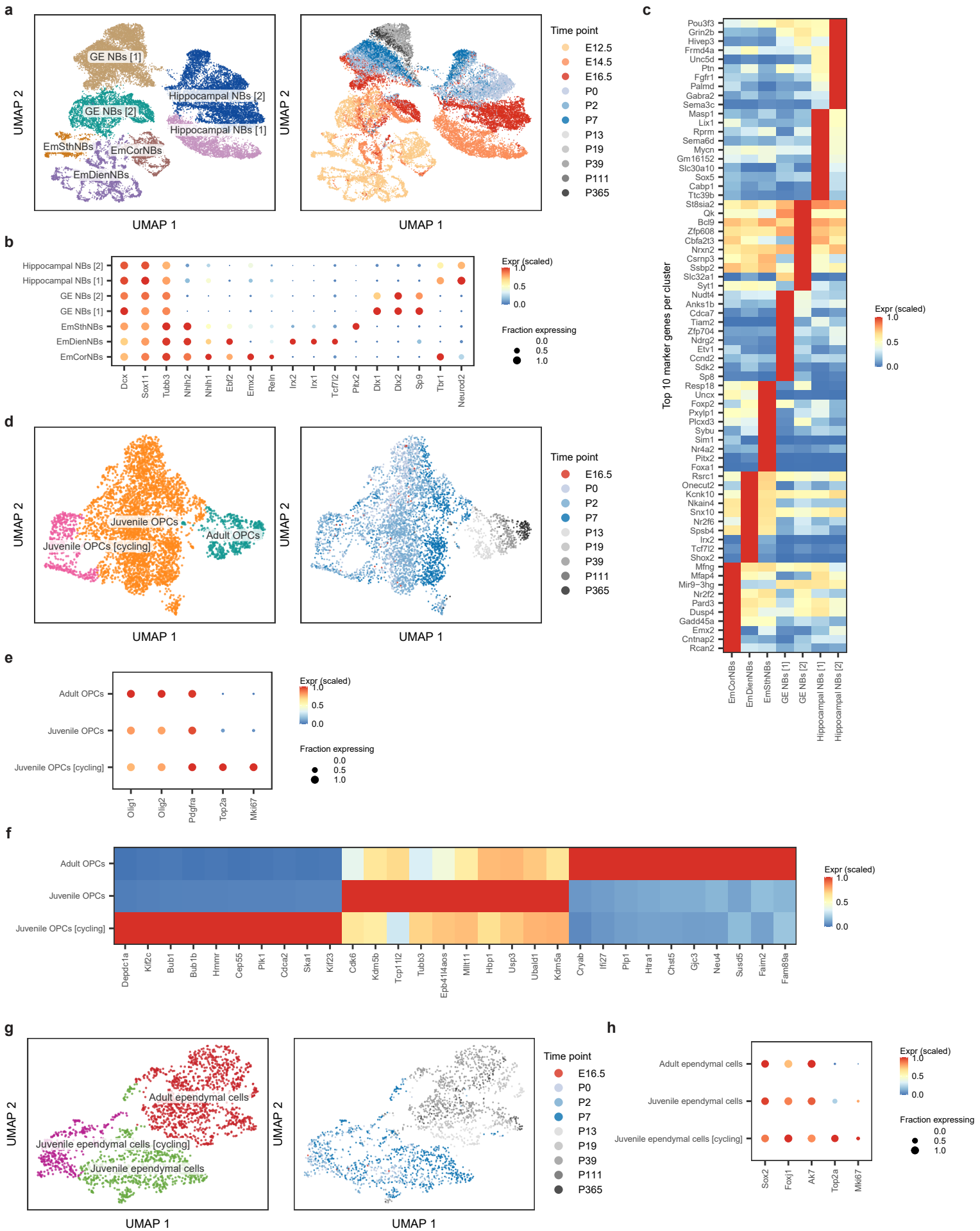
Timepoint	QC pass [%]	n cells post QC [GFP+ (Sox2)]	n cells post QC [GFP-]	n cells post QC [total]
E12.5	78.31	6188	4760	10948
E14.5	80.69	4533	4157	8690
E16.5	52.90	5847	2761	8608
P0	57.44	4908	4737	9645
P2	67.11	5019	5331	10350
P7	66.41	6294	7688	13982
P13	71.51	1762	1263	3025
P19	67.23	4558	3785	8343
P39	77.47	8008	4208	12216
P111	85.87	4351	4439	8790
P365	83.79	4461	3461	7922

b**c****e****d**

Supplementary Fig. 2 | Quality control and the Sox2/GFP analysis. **a**, Table summarizing some of the QC statistics for each timepoint in the mouse atlas. **b**, Violin plots of the number of genes/cell, UMIs/cell and fraction of mitochondrial reads/cell across the different samples. Colour bars indicate the sample type based on the FACS gating. **c**, Bar plot showing the normalized relative fraction of the Neuronal and Glial cell types grouped by timepoint. Colours correspond to the 2 cell types. The annotation is based on logistic regression from Zeisel et al., 2018 (see Fig. 1d). **d**, Bar plot showing the number of cells identified for each cell type in the dataset (see Fig. 1b). **e**, Left: two-dimensional UMAP visualization of the FACS GFP⁺/GFP⁻ gating. Shown on the right is the log₁₀-expression of Sox2 overlaid on the UMAP plot of the single cells collected from the various mouse brain samples. Each dot represents a single cell and the colour scale reflects the gene expression level. Source data are provided as a Source Data file. Abbreviations as in Fig. 1.



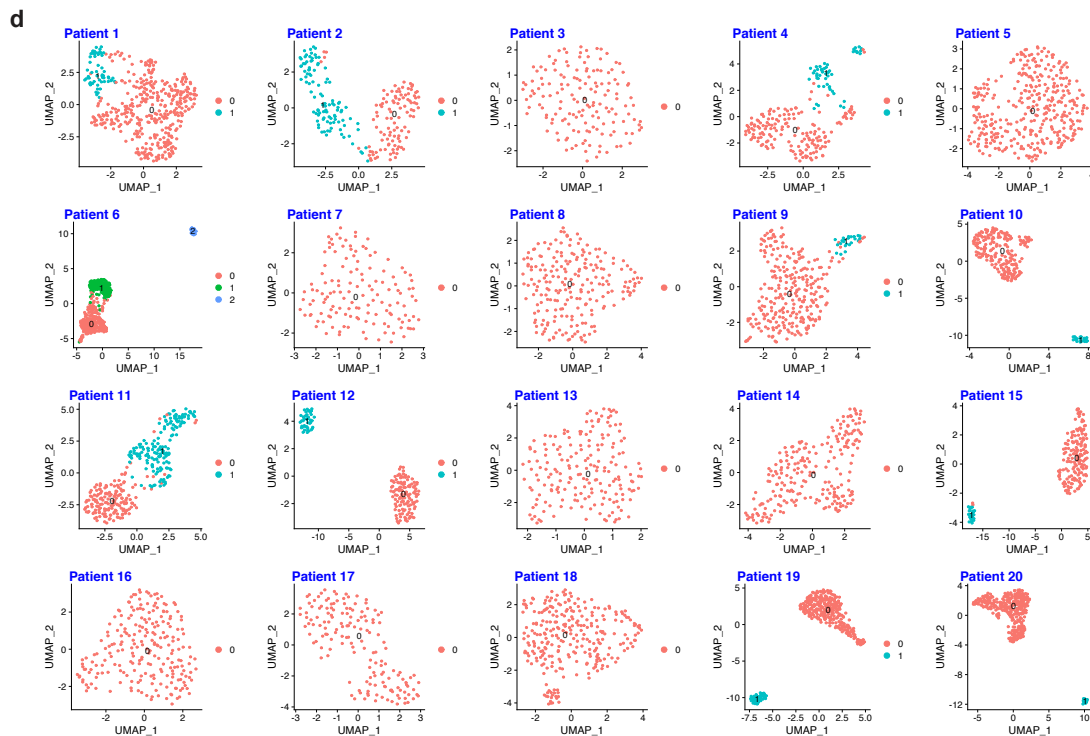
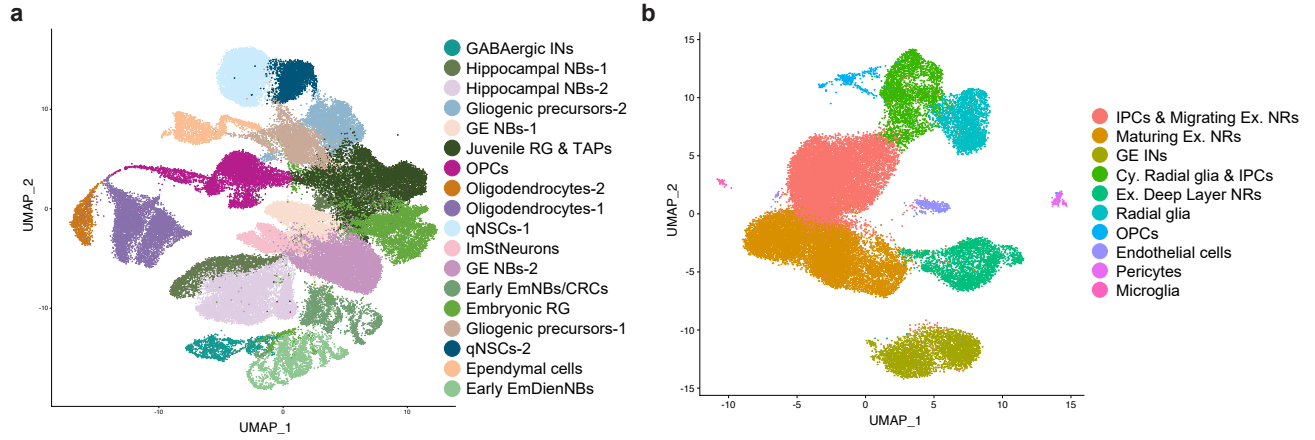
Supplementary Fig. 3 | a, Dot plot showing the normalized expression levels of lineage-specific marker genes used to annotate the clusters in Fig. 1b. The colour scale reflects the gene expression level and the dot size indicates the percentage of cells in each cluster expressing that gene. **b**, Heatmap of the top 20 DE marker genes identified per cluster from analyzing the clusters in Fig. 2a. Colour scale indicates the scaled mean expression in each cluster. **c**, Visualization of the FACS GFP⁺/GFP⁻ gating overlaid on the lineage tree of the neuronal/glia cells (see Fig. 2e). Each dot represents a single cell and the colour scale reflects the FACS gating GFP⁺/GFP⁻. **d**, UMAP plot of each of the four precursor populations identified in Fig. 2a with the cell cycle stages indicated by the colours. Each dot represents a single cell. Cycling stages were identified based on Cyclone (see Methods). The scale colours correspond to the cell cycle stages. **e**, Heatmap generated from the SCENIC analysis of the embryonic RG subtypes identified in Fig. 3a showing the top 10 TF regulons per cluster. Colour scale indicates the mean regulon score. Abbreviations as in Fig. 1.



Supplementary Fig. 4 | Temporal diversity of the lineage cell-types throughout forebrain development.

a, Left: two-dimensional UMAP visualization of the neuroblast clusters identified in the dataset from Fig. 1b. Each dot represents a single cell and the colours correspond to the distinct neuroblast subtypes. Right, UMAP plot of the cells coloured by timepoint. Each dot represents a single cell and the colours correspond to the different timepoints. **b**, Dot plot of the main marker genes used to differentiate/annotate the distinct neuroblast clusters. Dot size indicates the percentage of cells in each cluster expressing that gene. **c**, Heatmap of the top 10 DE marker genes identified per cluster from analyzing the clusters in (a). Colour scale indicates the scaled mean expression in each cluster. **d**, Left: two-dimensional UMAP visualization of the distinct OPC clusters identified in the dataset. Each dot represents a single cell and the colours correspond to the distinct clusters. Right: UMAP plot of the cells coloured by timepoint. Each dot represents a single cell and the colours correspond to the different timepoints. **e**, Dot plot of the main marker genes used to differentiate/annotate the distinct OPC clusters. Dot size indicates the percentage of cells in each cluster expressing that gene. **f**, Heatmap of the top 10 DE marker genes identified per cluster from analyzing the clusters (d). Colour scale indicates the scaled mean expression in each cluster. **g**, Left: two-dimensional UMAP visualization of ependymal cell clusters identified in the dataset. Each dot represents a single cell and the colours correspond to the distinct clusters. Right: UMAP plot of the cells coloured by timepoint. Each dot represents a single cell and the colours correspond to the different timepoints. **h**, Dot plot of the main marker genes used to identify ependymal cells in the dataset. Dot size indicates the percentage of cells in each cluster expressing that gene.

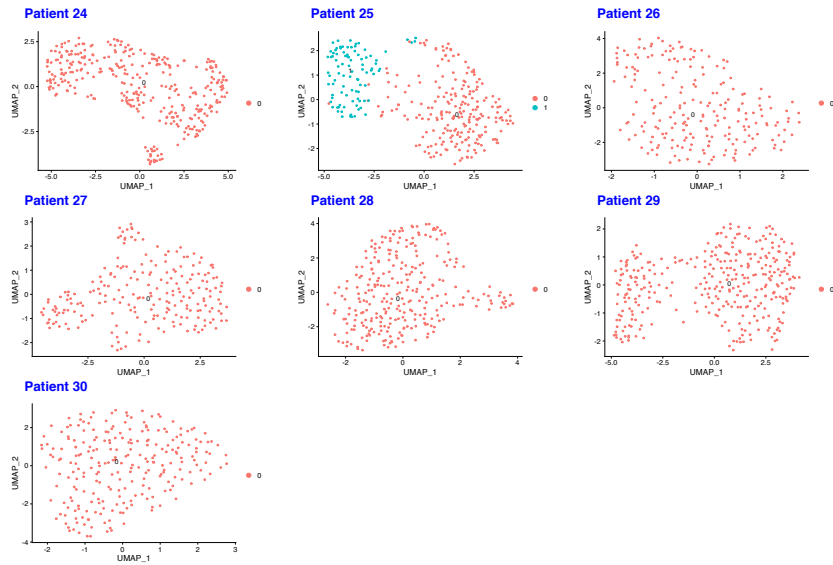
Abbreviations: EmThNBs: embryonic thalamic neuroblasts, EmCorNBs: embryonic cortical neuroblasts, EmSthNBs: embryonic subthalamic neuroblasts, EmDienNBs: embryonic diencephalon neuroblasts. Other abbreviations are as in Fig. 1.



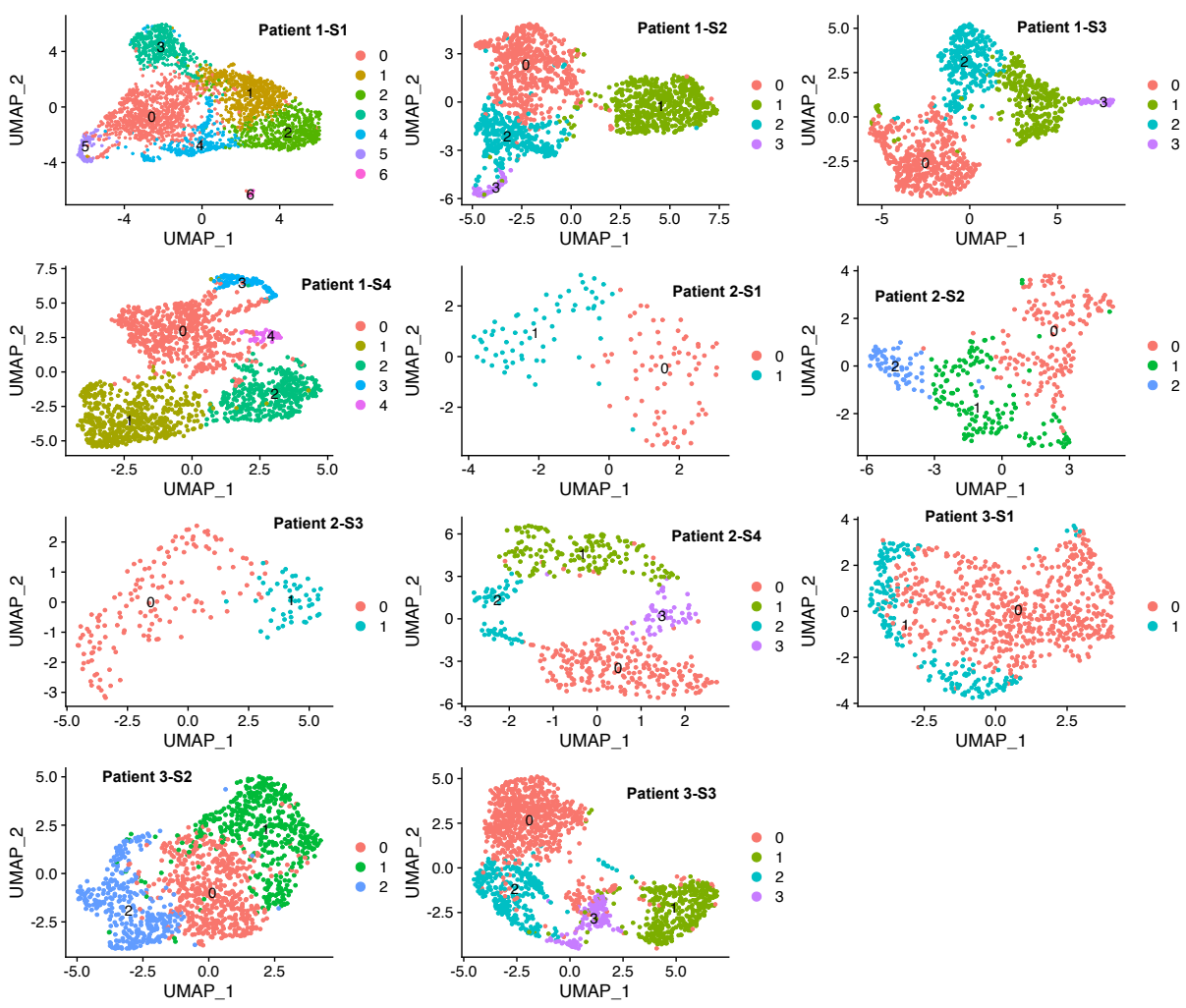
Supplementary Fig. 5 | Mapping human foetal scRNA-seq data to the mouse atlas reveals high similarities between the human foetal RG and the mouse embryonic and juvenile RG. **a**, Two-dimensional UMAP visualization of the clustered mouse atlas (after excluding the immune and vascular clusters) showing the neuronal and glial lineages which were used for the deconvolution analysis. Each dot represents a single cell and the colours correspond to the different clusters. **b**, Two-dimensional UMAP visualization of the human foetal dataset from Polioudakis et al., 2019 coloured by cell type. Each dot represents a single cell. **c**, Aligning the mouse atlas neuronal and glial clusters (x-axis) to the neuronal and glial cell types identified in the human foetal brain scRNA-seq data (y-axis) showing relative fraction of the mouse cell-types for each human cluster. The coloured cluster names indicate matching clusters between the mouse and human datasets. **d**, Clustering analysis of the scRNA-seq data from each patient from the Smart-seq2 adult GBM dataset (from Nefitel et al., 2019), which was used in the deconvolution analysis in Fig. 4a (see Methods and Supplementary Data 1). Each dot represents a single cell and colours correspond to the distinct clusters.

Abbreviations: Cy.: cycling, IPCs: intermediate progenitor cells, GE INs: ganglionic eminence interneurons, Ex. NRs: excitatory neurons. Other abbreviations are as in Fig. 4.

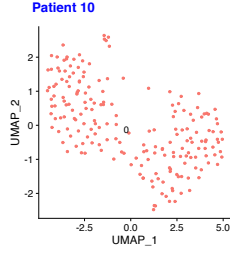
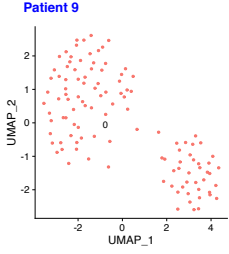
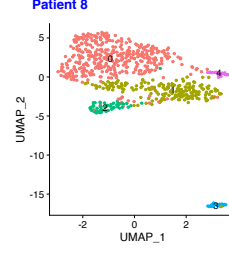
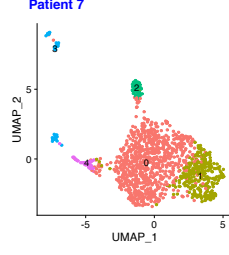
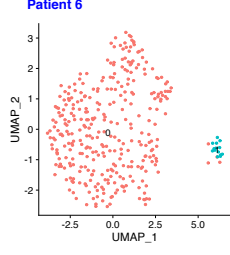
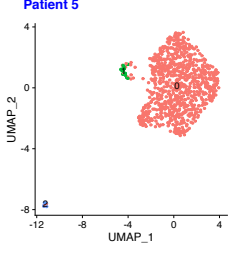
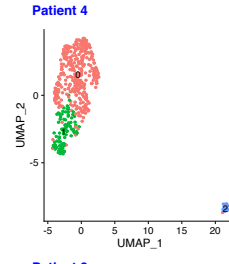
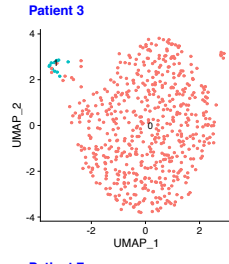
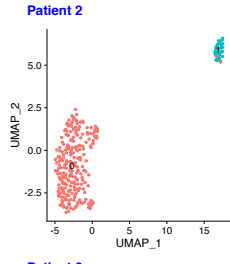
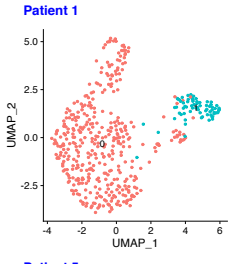
a



b

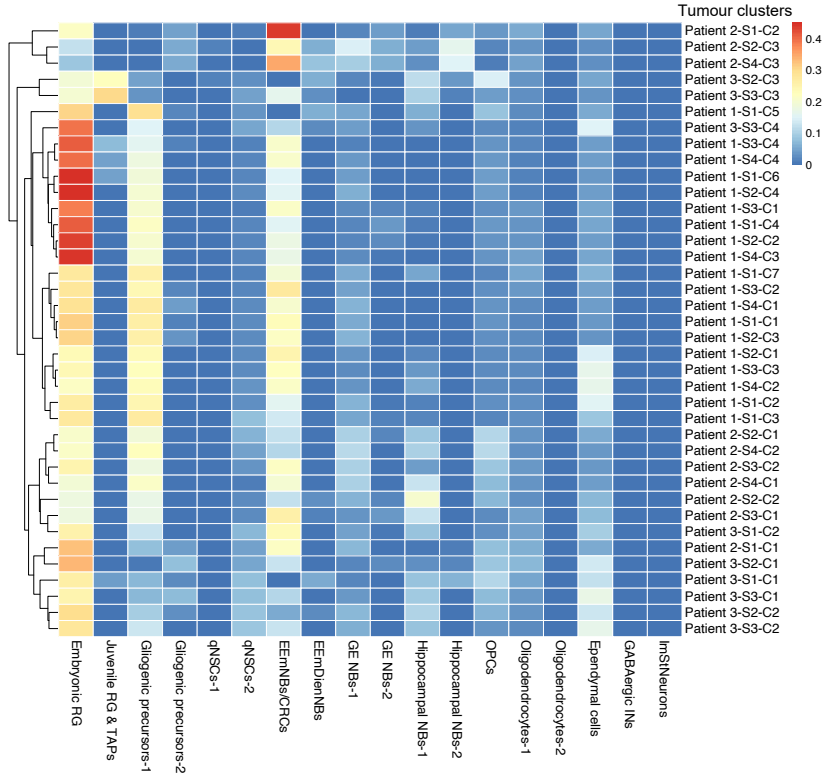


Supplementary Fig. 6 | a, Clustering analysis of the scRNA-seq data from each patient from the Smart-seq2 paediatric GBM dataset (from Neftel et al., 2019), which was used in the deconvolution analysis in Fig. 4. (see Methods and Supplementary Data 1). **b**, Clustering analysis of the scRNA-seq data from the GBM dataset (from Richards et al., 2021), which was used in the deconvolution analysis in Supplementary Fig. 8a (see Methods and Supplementary Data 1). Each patient sample is clustered separately and the clusters are denoted as e.g. “Patient#1-Sample#1-cluster#1” = “Patient 1-S1-C1” (see Supplementary Data 1). Normal brain and immune cells were excluded prior to the clustering analysis (based on the InferCNV analysis and immune markers expression). Each dot represents a single cell and colours correspond to the distinct clusters.

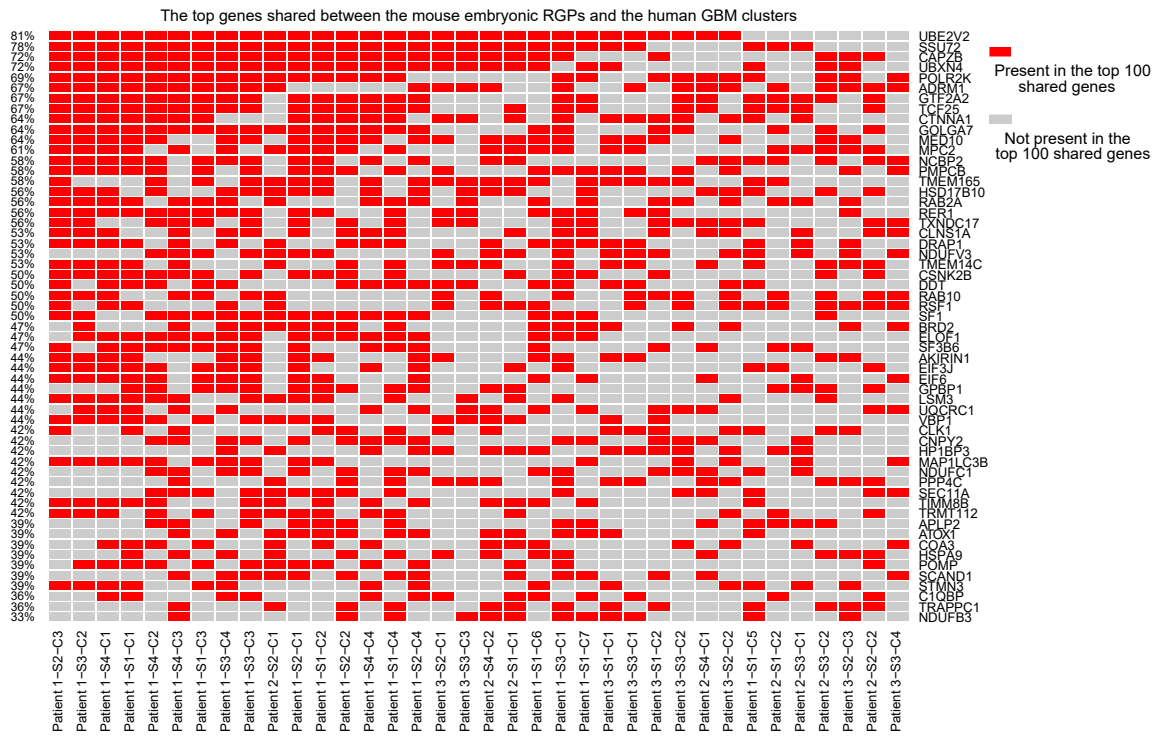


Supplementary Fig. 7 | Clustering analysis for each patient from the scRNA-seq of the IDH-mutant glioma dataset (Venteicher et al., 2017), which was used in the deconvolution analysis in Fig. 5a. See Methods and Supplementary Data 1.

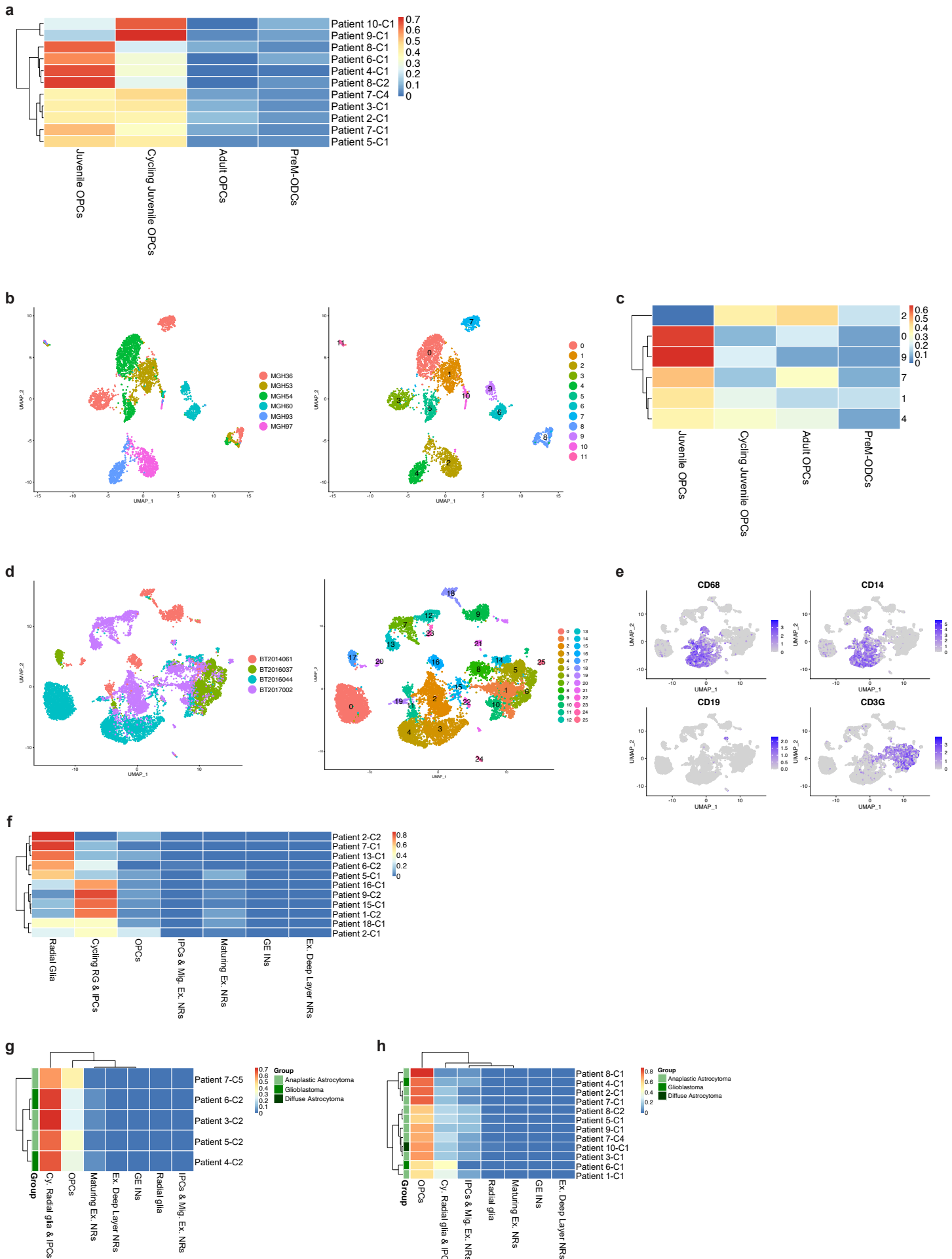
a



b

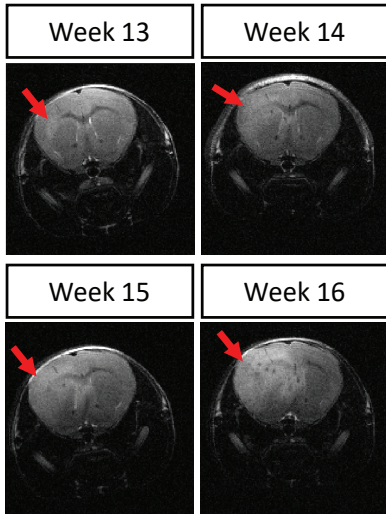
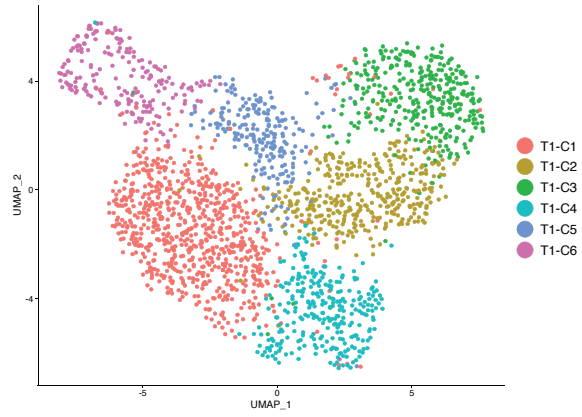
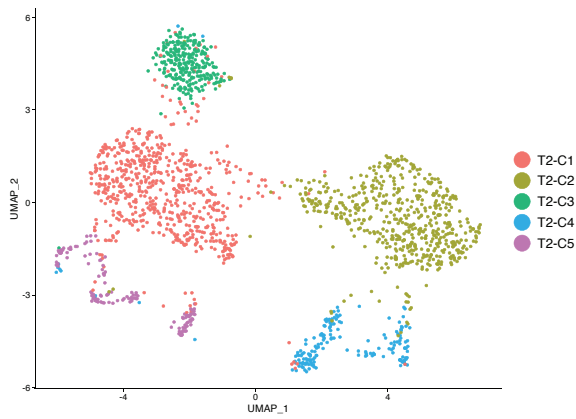
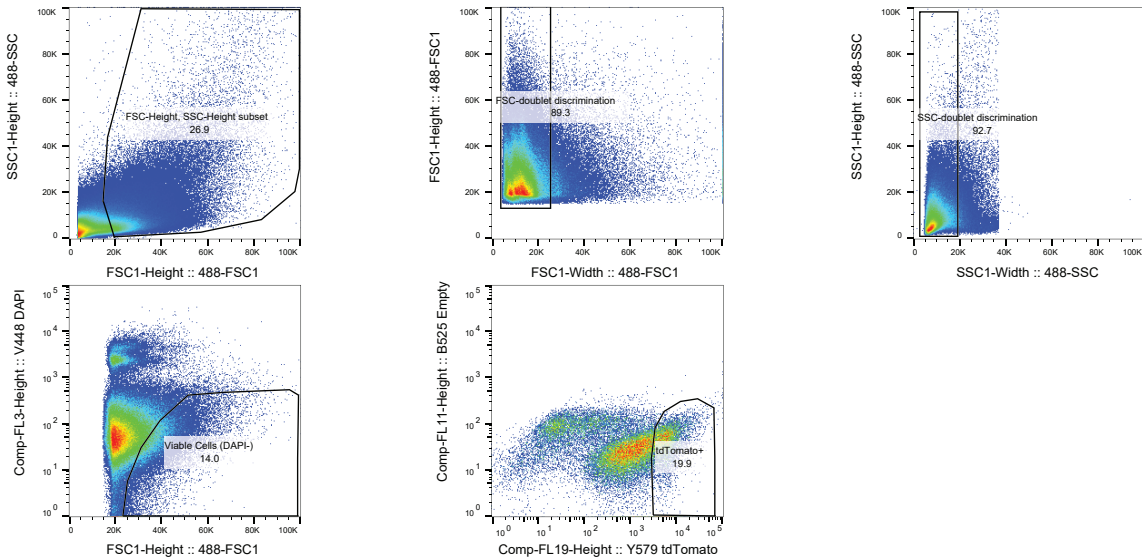


Supplementary Fig. 8 | Identifying the genes shared between the GBM cells and the matching embryonic precursors. **a**, Deconvolution analysis heatmap of malignant clusters from 11 scRNA-seq samples obtained from 3 adult GBM patients from Richards et al., 2021 showing the estimated relative fraction of the mouse cell-types for each patient cluster (see Methods). Each patient sample was clustered separately (see patient clustering in Supplementary Fig. 6b) and the clusters are denoted as e.g. "Patient#1-Sample#1-cluster#1" = "Patient 1-S1-C1" (see Supplementary Data 1). **b**, A plot showing the top shared genes between the mouse embryonic RG cluster and the matching patient clusters from the deconvolution analysis in panel (a), the plot shows the genes that are present in the top 100 genes shared between the embryonic RG cluster and at least 15 or more individual patient tumour clusters (see Methods and the full list of shared genes in Supplementary Data 2). The red bars indicate that the gene is in the top 100 genes shared between the patient tumour cluster and the mouse embryonic RG cluster. The numbers on the left indicate the percentage each gene is commonly shared in the total number of patient clusters. Abbreviations as in Fig. 4.



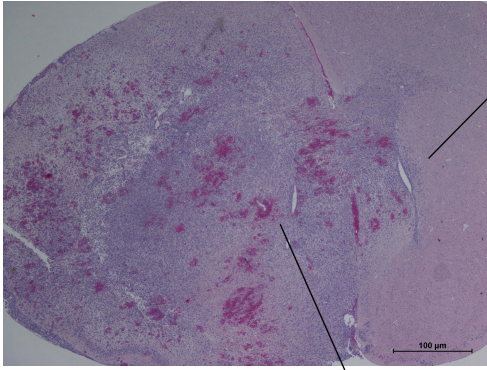
Supplementary Fig. 9 | The OPC-matching clusters from IDG and ODG patients map more closely with juvenile rather than adult OPCs. **a**, Matching of the IDG patient clusters, which showed an OPC-type identity in Fig. 5a, against the cell types identified in the mouse OPC cluster from Supplementary Fig. 5a. **b**, Clustering analysis of scRNA-seq data from 6 ODG patients coloured by the patient identity (left) and distinct clusters (right). This clustering was used in the deconvolution analysis in Fig. 5b. **c**, Matching of the ODG patient clusters, which showed an OPC-type identity in Fig. 5b, against the cell types identified in the mouse OPC cluster from Supplementary Fig. 5a. **d**, Clustering analysis and visualization of scRNA-seq data from 4 supratentorial ependymoma patients. Each dot represents a single cell and the colours correspond to the distinct clusters (left) and the patient identities (right). This clustering was used in the deconvolution analysis in Fig. 5c. **e**, UMAP showing normalized expression levels (colour) of immune cell-specific markers to distinguish the immune clusters/microenvironment from the tumour clusters. **f**, Deconvolution analysis of the IDH-wildtype GBM patient clusters which showed an embryonic RG-type identity in Fig. 4a, against the neuronal/glial cell types identified in the human foetal dataset in Supplementary Fig. 5b. **g**, Matching of the IDG patient clusters, which showed an embryonic RG-type identity in Fig. 5a, against the neuronal/glial cell types identified in the human foetal dataset in Supplementary Fig. 5b. **h**, Matching of the IDG patient clusters, which showed an OPC-type identity in Fig. 5a, against the neuronal/glial cell types identified in the human foetal dataset in Supplementary Fig. 5b.

Abbreviations as in Fig. 4 and Supplementary Fig. 5.

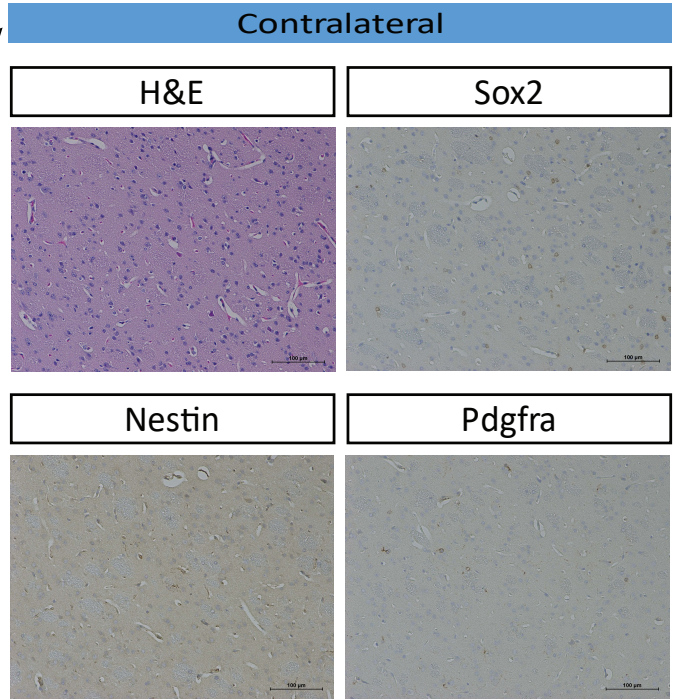
a**b****c****d**

Supplementary Fig. 10 | **a**, MR images of a mutant mouse brain at 13, 14, 15 and 16 weeks of age showing the growth of a tumour encompassing the left hemisphere (red arrows). **b, c**, Clustering analysis of the malignant cells from the mouse tumour replicate 1 (b) and 2 (c), which was used in the deconvolution analysis for Fig. 7. Each dot represents a single cell and colours correspond to the distinct clusters. **d**, FACS plots of the collection strategy of the tdTomato+ cells from the mouse tumour sample in Fig. 7.

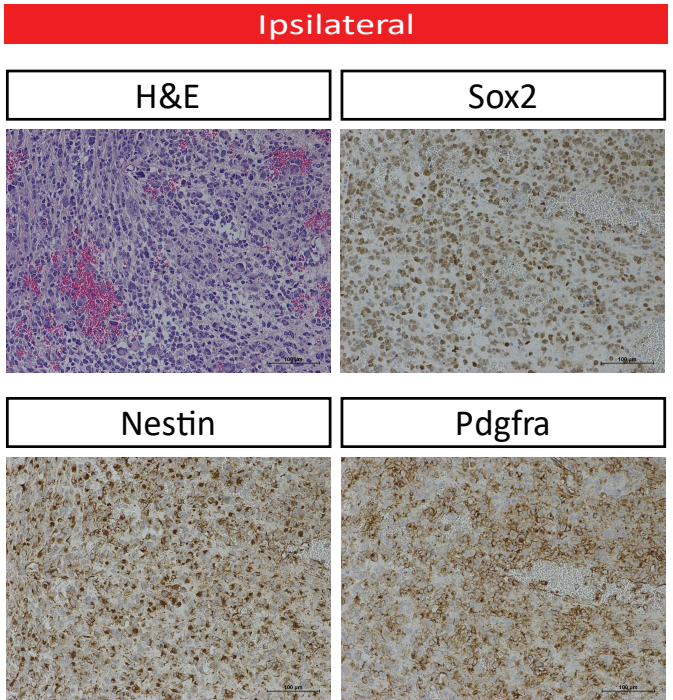
a



b



c



Supplementary Fig. 11 | a, H&E-stained section of the mouse brain in Fig. 7b. Scale bar, 100 μ m. **b**, H&E-staining and immunostaining for the three proteins, Sox2, Nestin and Pdgfra, in both the contralateral (top) and tumour/ipsilateral (bottom) hemispheres. Scale bar, 100 μ m.